Sawtooth Stabilization by Localized Electron Cyclotron Heating in a Tokamak Plasma

K. Hanada, H. Tanaka,[a] M. Iida, S. Ide,[b] T. Minami, M. Nakamura,[c] T. Maekawa, Y. Terumichi, and S. Tanaka

Department of Physics, Faculty of Science, Kyoto University, Kyoto, Japan

M. Yamada, J. Manickam, and R. B. White

Plasma Physics Laboratory, Princeton University, Princeton, New Jersey 08543

(Received 5 October 1990)

Sawtooth oscillations (STO) in the Ohmically heated WT-3 tokamak are strongly modified or suppressed by localized electron-cyclotron-resonance heating (ECH) near the $q=1$ surface, where q refers to the safety factor. The effect of ECH is much stronger when it is applied on the high-field side as compared to the low-field side. Complete suppression of STO is achieved for the duration of the ECH, in most cases, when it is applied on the high-field side of a low-density plasma, provided the ECH power exceeds a threshold value. STO stabilization is attributed to a modification of the current-density profile by hot electrons generated by ECH, which reduces the shear in the $q=1$ region.

PACS numbers: 52.50.Gj, 52.35.Hr, 52.35.Py, 52.55.Fa

Sawtooth oscillations (STO) in tokamaks have long been the subject of intense study. Recently it has been recognized that they can be stabilized by a variety of means, including lower-hybrid current drive,[1-4] ion-cyclotron-range-of-frequencies (ICRF) heating,[5] and electron-cyclotron-resonance heating[6-9] (ECH). Several models[10-12] have been proposed as possible stabilization mechanisms. However, a comparison of these models with experiments has been inconclusive, partly due to the difficulty of monitoring and or controlling the plasma parameters near the $q=1$ surface, where q refers to the plasma safety factor. In the WT-3 tokamak, STO are observed to be strongly modified and/or stabilized by ECH. The sharply localized nature of the ECH provides an effective tool for modifying plasma parameters locally near the $q=1$ surface. These observations as well as plausible theoretical explanations for the stabilization are the subject of this Letter.

The experiments were carried out in the WT-3 tokamak,[13] with major and minor radii of $R=65$ and $a=20$ cm, respectively. The toroidal field was $B_T \leq 1.75$ T, and the plasma current was $I_p \leq 150$ kA. Microwaves from a gyrotron ($\omega/2\pi=56$ GHz, $P_{ECH} \leq 200$ kW) were transferred through circular wave guides to a Vlasov antenna with an elliptic reflector placed along the major radius and injected into the plasma from the low-field side. This sharply focused wave, propagating as the X mode with an angle of $\theta=88°$ to the toroidal field, is absorbed at the second-harmonic ECH resonance layer, r_{ECH}. In the present operational condition, the ECH is not considered to cause direct current drive at the resonance region.

Sawtooth oscillations were observed when the current was such that the safety factor at the limiter was in the range $q_L=2.2$–6.0. The sawtooth period τ_s as well as the amplitude increase when the ECH power P_{ECH} is applied. These modifications of the STO are very sensitive to the field B_T which determines the location where the ECH is localized. The ECH power is held constant and B_T is adjusted so that the resonance occurs at different surfaces; the geometric configuration is shown in Fig.

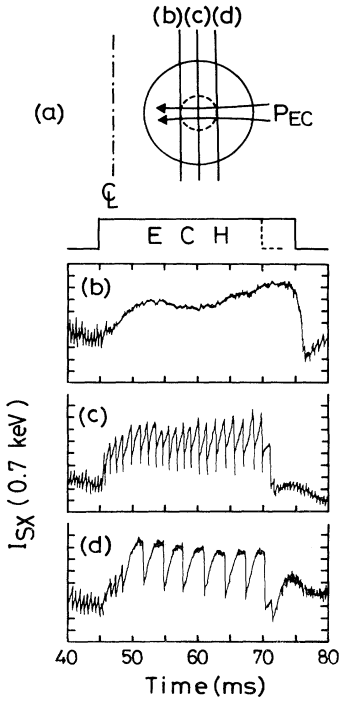

FIG. 1. (a) Schematic of the wave trajectory and ECH layers r_{ECH} shown as vertical lines for the three cases (b), (c), and (d) shown below. The $q=1$ surface is shown as a dashed circle. Evolution of the soft-x-ray signal $I_{sx}(0.7$ keV) for (b) ECH at $q=1$ on the high-field side ($B_T=0.93$ T), (c) on-axis heating ($B_T=1.02$ T), and (d) on the low-field side of $q=1$ ($B_T=1.08$ T), for $q_L=3.4$, $I_p=83$–100 kA, and $P_{ECH}=213$ kW.

1(a), while the changes in the soft-x-ray (SXR) signal I_{sx} due to the ECH are shown in Figs. 1(b)–1(d). When the ECH is at the $q=1$ surface on the high-field side (HFS), Fig. 1(b), the sawtooth oscillations are completely stabilized. When the heating occurs on the low-field side (LFS) of the same $q=1$ surface, τ_s increases to a value greater than the energy confinement time τ_e ($\tau_s=3$ ms, $\tau_e=1$ ms), and the amplitude saturates, Fig. 1(d). In contrast, when the heating occurs away from the $q=1$ surface, STO was little affected. When ECH is applied at the magnetic axis, I_{sx} ramps up sharply and drops deeply during the crash phase, Fig. 1(c). These observations clearly indicate the critical importance of the location of the application of ECH. Other effects are easily excluded, since the plasmas in the Ohmically heated (OH) phase are essentially similar. [With ECH at $r_{q=1}$ on the LFS, the electron density decreases slightly, $n_e=(7\rightarrow 6)\times 10^{12}$ cm^{-3}, and the temperature as measured by Thomson scattering increases, $T_{e\perp}(0)=510\rightarrow 670$ eV, resulting in a decrease of the loop voltage, $V_L=1.5\rightarrow 0.8$ V, while the plasma current was held constant at $I_p=80$ kA ($q_L=4.3$). There was no change in the O V impurity line emission.]

These results are shown in greater detail in Figs. 2(a) and 2(b). Figure 2(a) shows the dependence of τ_s on $r_{2\Omega_e}$, which is varied by changing B_T, without and with ECH. In the former case we observe that there is no significant variation at all. On the other hand, τ_s has two resonance values when B_T is such that the ECH occurs at $r_{q=1}$, where τ_s increases significantly. When $r_{ECH}=r_{q=1}$ on the HFS, τ_s is increased and complete stabilization is observed. On the other hand, when the heating is on the LFS, τ_s is increased substantially but stabilization is not observed. These results are complemented by the corresponding variation in the amplitude, Fig. 2(b), which shows the peaking of the amplitude when the ECH is on axis and at $r_{q=1}$. The $q=1$ radius can be estimated from computer tomographic reconstructed images of SXR emissivity at the crash phase, and also from the measured T_e profiles; as often noted before, $r_{q=1}$ is a little larger than r_{inv}, since the latter is determined by the spatial variation of the SXR signal integrated along the line of sight.

We emphasize that there was very little effect of ECH on the sawtooth when $r_{2\Omega_e}>r_{q=1}$. If the main reason for STO stabilization is $q_{axis}>1$, one would expect the same strong effect even when $r_{2\Omega_e}>r_{q=1}$, and we could not explain the sharp observed resonance at $r_{q=1}$. Only a slight incremental change of r_{inv} was detected with a high-power ECH for $2.6\leq q_L\lesssim 4.5$ and the global magnetic parameter (i.e., the self-inductance l_i) did not exhibit an evidence for a major change of $j(r)$ or $q(r)$.

In addition to the influence of B_T, which determines the location of the ECH, other plasma parameters play an important role as well. These include the power of the ECH P_{ECH} and the electron density n_e. The dependence on P_{ECH} is shown in Fig. 3, where we have plotted τ_s as a function of P_{ECH}/P_{OH}. We observe that there is an initial linear phase where τ_s increases linearly, and at larger value of P_{ECH}/P_{OH} there is a rapid nonlinear increase resulting in complete stabilization. This occurs at $P_{ECH}/P_{OH}\simeq 3.5$ for the particular set of plasma conditions of Fig. 3, $q_L=3.4$, $n_e=5\times 10^{12}$ cm^{-3} when the ECH is at $r_{q=1}$ on the HFS. In contrast, τ_s just in-

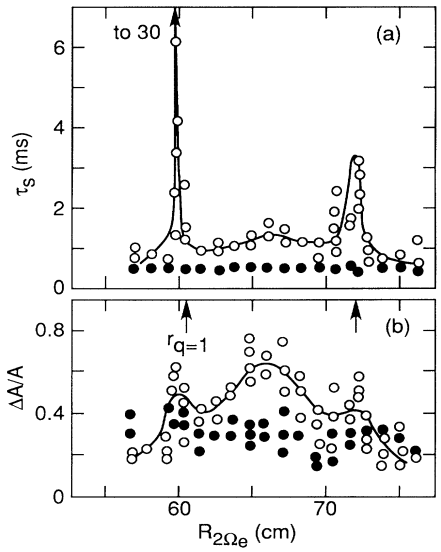

FIG. 2. (a) The sawtooth period τ_s and (b) relative amplitude $\Delta A/A$ plotted vs r_{ECH} (or B_T) with P_{ECH} (open circles) and without P_{ECH} (solid circle); $q_L=3.4$. Note that τ_s reaches 30 ms, the duration of the ECH, when $r_{ECH}=r_{q=1}$ on the high-field side.

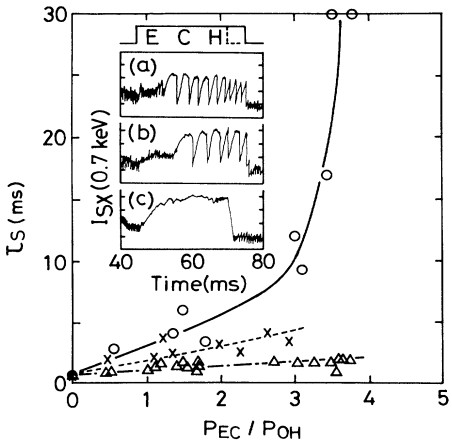

FIG. 3. τ_s vs normalized ECH power, P_{ECH}/P_{OH}, for the $q=1$ surface on the HFS (open circles), low-field side (crosses), and for on-axis heating (triangles). Insets: Temporal evolution of the SXR signal above 0.75 keV for various ECH power values: (a) $P_{ECH}=46$, (b) 123, and (c) 213 kW; the ECH was on the HFS, with $I_p=80$ kA, $B_T=0.91$ T, $n_e=5\times 10^{12}$ cm^{-3}, and $q_L=3.4$.

creases linearly with P_{ECH} when the ECH is on the LFS or at the magnetic axis. The threshold value decreases when q_L increases. When $q_L \sim 4.7$ the critical power for stabilization is $P_{ECH}/P_{OH} \sim 1$. It is interesting to note that at these high-q_L values complete stabilization of the STO is possible even when ECH is applied on the LFS. In this case the threshold power on the LFS is 1.7 times larger than the threshold on the HFS.

The electron density also plays a critical role. The period τ_s increases abruptly when n_e decreases below $n_e = 6 \times 10^{12}$ cm^{-3}, complete suppression is obtained when $n_e \sim 5 \times 10^{12}$ cm^{-3}, and the ECH is at $r_{q=1}$ on the HFS. Concomitantly, the x-ray energy spectra show a high-energy tail indicating the presence of a hot-electron population with $T_{eh} \simeq 60$ keV extending up to 300 keV in these low-density plasmas. In the absence of ECH ($T_e \sim 0.5$ keV), hot-electron tails are not observed. The SXR emission from the thermal electrons above 0.9 keV increases with density regardless of the presence or absence of ECH.

These observations suggest that the high-energy tail electrons generated by ECH in the low-density regime may be responsible for the stabilization of the STO. However, it must be noted that these hot electrons are generated equally profusely when the ECH is applied either at the axis or at the LFS of the $q=1$ surface. As such they cannot account entirely for the stabilization of the sawtooth, but might contribute to the effect. Here, we propose that the stabilization is due to a modification of the current profile in such a manner as to lower the shear at the $q=1$ surface, thus stabilizing the resistive $m/n=1/1$ mode.[10] Specifically, we suggest that when ECH is applied $T_{e\perp}$ increases ($\delta T_{e\perp}/T_{e\perp} \simeq 0.3$), and the electron collisionality and hence the plasma resistivity is reduced, driving more current in this region, Figs. 4 and 5. This incremental change of the current density would result in a local reduction of the shear,

$$s = \frac{2}{q}\frac{dq}{d\psi}\frac{V}{dV/d\psi},$$

where ψ refers to the poloidal flux, and V refers to the plasma volume enclosed by the surface. We note that this is the toroidal equivalent of $s = (r/q)dq/dr$. If this reduction in s occurs at the $q=1$ surface, it will have a stabilizing effect on the $m/n=1/1$ resistive mode which plays an important role in STO.

We have modeled this using the PEST code. We start with a current profile that smoothly vanishes at the plasma edge with $q_{axis}=0.83$, and $q_L=3.37$, and has the $q=1$ surface at an average radius of 0.35 of the plasma minor radius; a parabolic pressure profile is chosen. Although q_{axis} could not be measured accurately, the experimental evidence on other devices[4,5] suggests that q_{axis} is less than unity before and during the sawtooth stabilization period. Furthermore, in the present experiment, we expect $q_{axis} < 1$ due to the absence of an adequate mechanism for broadening the current profile.[5] We determine the stability of this model equilibrium to the ideal and resistive $m/n=1/1$ modes. The q profile is modified locally near the $q=1$ surface in a manner which reduces the shear at that surface, and a new equilibrium is computed.

The stability limits of such a sequence of equilibria at different values of β_{pol} are shown in Fig. 4(a). In the initial OH phase the plasma is unstable to the resistive

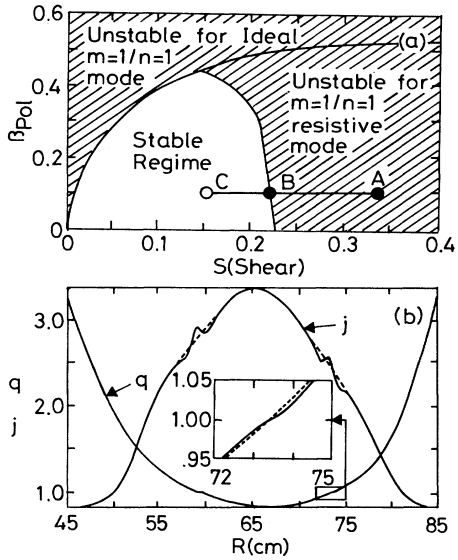

FIG. 4. (a) Stability diagram for the $m/n=1/1$ mode in WT-3, with respect to the shear s and β_{pol}. The two curves show the stability boundaries for the resistive and ideal instability. As the ECH power is increased the shear is reduced and the plasma moves from an unstable point (A) without ECH, to a marginal point (B) with ECH at threshold power, to a stable point (C) with substantial ECH power. (b) The current density j and q profiles across the plasma midplane without ECH (dashed curves) and with ECH (solid curves). Inset: A magnification of the $q \simeq 1$ region to show the reduction of the shear when the ECH was in use.

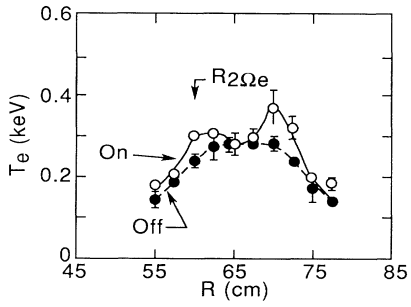

FIG. 5. Radial T_e profile measured by Thomson scattering with (open circles) and without (solid circles) ECH near the $q=1$ region. Magnetic axis is at $r=66$ cm and ECH is at $r=60$ cm.

mode (A), and as the ECH is applied the shear is reduced and the plasma is at marginal stability at (B); further heating reduces the shear further and stabilizes the mode completely (C). The current profile at this point shows a local peak near the $q=1$ surface and is associated with a reduction of the local shear as indicated in Fig. 4(b). Thus we attribute the suppression of the sawteeth to a stabilization of the $m/n=1/1$ mode by profile modification. An evidence of enhanced electron temperature at the cyclotron resonance flux surface is attained using Thomson scattering diagnostics with ECH applied on other than the magnetic axis. Figure 5 depicts the $T_e(r)$ profile for a high-power ECH applied on $r_{q=1}$. Based on these T_e profiles, the current-density perturbation of $\Delta j/j_0 > 0.2$ is easily expected since $V_{\text{loop}}(r) \simeq$const in the steady-state discharges. On the other hand, in our theoretical model, the required current modification for stabilization is $\Delta j/j > 0.05$, consistent with the observed result.

To explain *the differences when heating on the HFS and LFS,* we note that when ECH is applied on the HFS, the high-energy electrons can traverse most of the surface enhancing a locally peaked current profile on the entire surface. In contrast, when the ECH is applied on the LFS, many of the high-energy electrons are easily trapped in the "banana region" and do not contribute to an enhancement of the current density. As a result there is a smaller influence on the shear and hence the stability when heating on the LFS.

As indicated earlier, in addition to the effects of the high-energy electrons on the shear through the current profile, we might expect an energetic particle stabilization effect as discussed by White and co-workers.[11,12] Although the stability window discussed in Ref. 12 does not exist in the present experiment, since $\beta_p \ll 1$ and $\omega_A > \omega_e^*$, there is still a stabilizing effect from the high-energy electrons which are precessing much faster than the background diamagnetic velocity. Here $\omega_{de} > \omega_e^*/2$, where $\omega_{de} = W_\perp/erRB_T$, and $\omega_e^* = (k_\theta/eB_T)\nabla p/n_0$. This criterion can be written as $W_\perp > R\nabla p/n_0 \sim T_e R/a \sim 1.5$ keV ($T_e = 0.5$ keV) and is well fulfilled, since the measured hard-x-ray temperature is $T_{eh} \sim 60$ keV. However, this stabilization mechanism cannot explain why the effect is stronger for the HFS heating compared to the LFS heating.

In conclusion, we have found a significant effect of stabilization of STO due to ECH when it is applied near the $q=1$ surface. This effect is much stronger when the ECH is applied on the high-field side and it is consistent with our theoretical model. There is a power threshold above which complete stabilization is obtained; below that the sawtooth period increases linearly. Similarly stabilization occurs only below a density threshold. The stabilization is attributable to a local reduction of the shear near the $q=1$ surface with some contribution due to energetic particle effects. This latter effect may be similar to that observed with ICRF heating in JET and TFTR.[14] These results also suggest that STO may be controlled effectively with ECH at the $q=1$ surface, especially by application on the high-field side.

The authors appreciate many valuable discussions with Dr. A. Kritz, Dr. K. McGuire, Dr. W. Stodiek, and Dr. W. Tang. One of the authors (M.Y.) thanks the Japan Society for Promotion of Science for their support during his stay at Kyoto University. This work was supported by a Grant-in-Aid of Scientific Research from the Ministry of Education in Japan and U.S. Department of Energy, under Contract No. DE-ACO2-76CH03073.

[a]Present address: Physics Laboratory, College of Liberal Arts and Science, Kyoto University.

[b]Present address: Japan Atomic Energy Research Institute, Naka Fusion Research Establishment, Ibaraki-ken, Japan.

[c]Present address: Osaka Institute of Technology, Osaka, Japan.

[1]F. X. Soldner *et al.*, Phys. Rev. Lett. **57**, 1137 (1986).

[2]T. K. Chu *et al.*, Nucl. Fusion **26**, 666 (1986).

[3]K. McCormick *et al.*, Phys. Rev. Lett. **58**, 491 (1987); S. Knowlton *et al.*, Nucl. Fusion **28**, 99 (1988); M. Iida *et al.*, J. Phys. Soc. Jpn. **57**, 3661 (1988).

[4]JT-60 Team, I. Aoki *et al.*, Plasma Phys. Controlled Fusion **31**, 1597 (1989).

[5]D. J. Campbell *et al.*, Phys. Rev. Lett. **60**, 2148 (1988).

[6]G. A. Bobrovskii *et al.*, Fiz. Plazmy **13**, 1155 (1987) [Sov. J. Plasma Phys. **13**, 665 (1987)].

[7]TFR Group, M. H. Achard *et al.*, Nucl. Fusion **28**, 1995 (1988).

[8]R. T. Snider *et al.*, Phys. Fluids B **1**, 404 (1989).

[9]Y. Terumichi *et al.*, in *Proceedings of the Eighth Topical Conference on RF Power in Plasmas, Irvine* (Univ. of California, Irvine, 1989), p. 88.

[10]H. Soltwisch *et al.*, in *Proceedings of the Tenth International Conference on Plasma Physics and Controlled Nuclear Fusion Research, Kyoto, 1986* (IAEA, Vienna, 1987), Vol. 1, p. 263.

[11]R. B. White *et al.*, Phys. Rev. Lett. **60**, 2038 (1988).

[12]R. B. White *et al.*, Phys. Rev. Lett. **62**, 539 (1989).

[13]H. Tanaka *et al.*, Phys. Rev. Lett. **60**, 1033 (1988).

[14]J. C. Hosea *et al.*, in Proceedings of the Joint Varenna-Lausanne International Workshop on Theory of Fusion Plasmas, Varenna, 27–31 August 1990 (to be published).